Electronic Supplementary Material (ESI) for Molecular Systems Design & Engineering.
This journal is © The Royal Society of Chemistry 2016

Molecular Engineering of Fluorescein Dyes as Complementary Absorbers in Dye Co-sensitized Solar Cells: Electronic Supplementary Information

Giulio Pepe[a], Jacqueline M. Cole[a,b,c,d]*, Paul G. Waddell[a,e,1], Joseph R. D. Griffiths[a]

[a] *Cavendish Laboratory, University of Cambridge, J. J. Thomson Avenue, Cambridge, CB3 0HE, UK*

[b] *ISIS Neutron and Muon Source, STFC Rutherford Appleton Laboratory, Harwell Science and Innovation Campus, Didcot, Oxfordshire, OX11 0QX. UK*

[c] *Argonne National Laboratory, 9700 S. Cass Avenue, Argonne, IL 60439, USA.*

[d] *Department of Chemical Engineering and Biotechnology, University of Cambridge, Charles Babbage Road, Cambridge, CB3 0FS. UK*

[e] *Australian Nuclear Science and Technology Organisation, Lucas Heights, New South Wales, 2234, Australia*

* *E-mail: jmc61@cam.ac.uk (J. M. Cole)*

[1] Current address: School of Chemistry, Newcastle University, Newcastle upon Tyne, NE1 7RU. UK.

Table of Contents

S.1 X-Ray Diffraction S2
S.2 Nuclear Magnetic Resonance S3
S.3 UV/vis absorption spectroscopy S6
S.4 Computational Studies S7

S.1 X-Ray Diffraction

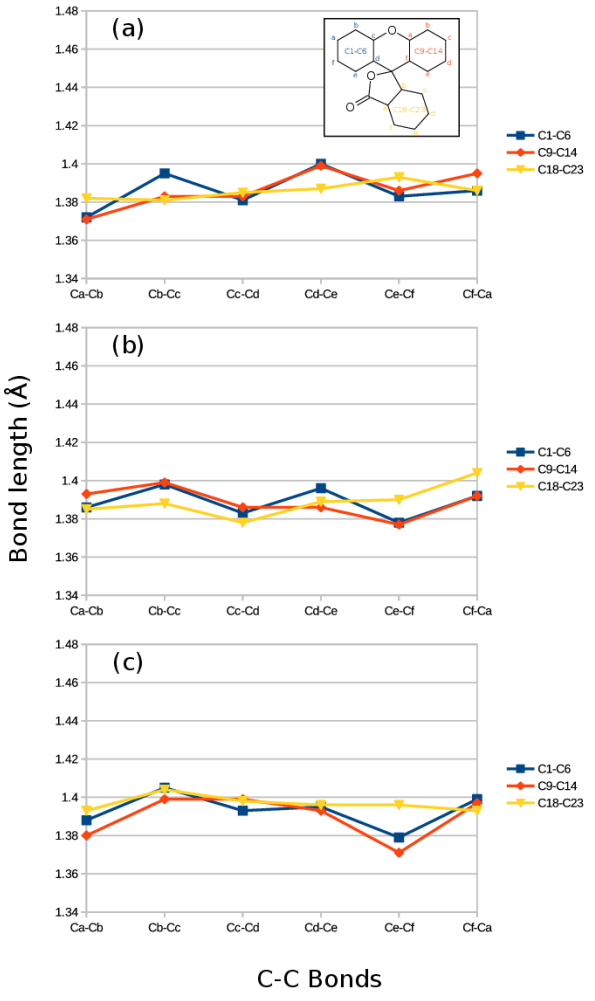

Figure S.1: Bond lengths for the carbon atoms in the arene rings of (a) **3**, (b) **4**, and (c) the 5-substituted (para) component of **5** from the crystal structures. The rings have been identified by their labels of carbon atoms for all three structures and highlighted in the inset chemical schematic: xanthene rings (C1-C6 and C9-C14) and benzoxolane ring (C18-C23).

S.2 Nuclear Magnetic Resonance

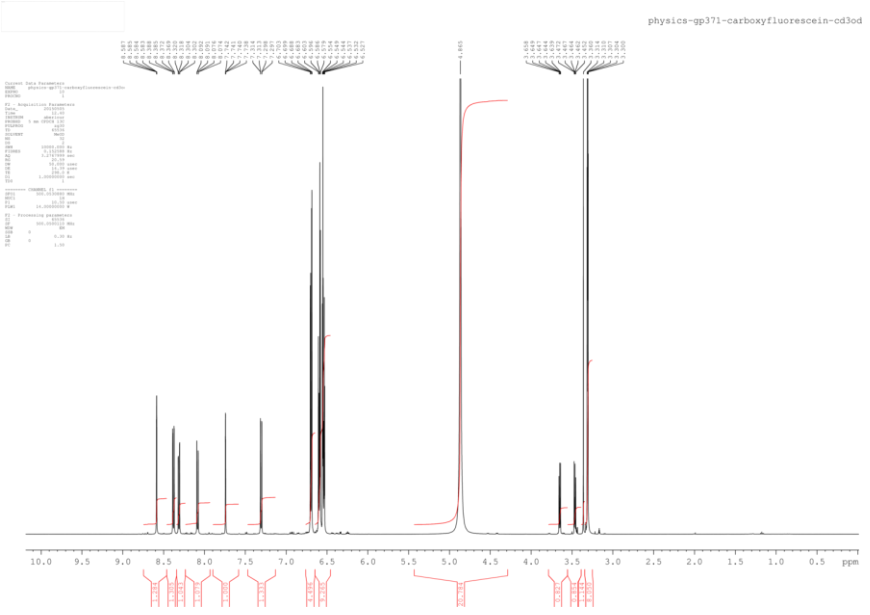

Figure S.2: ^{1}H NMR spectrum of **2** in deuterated methanol.

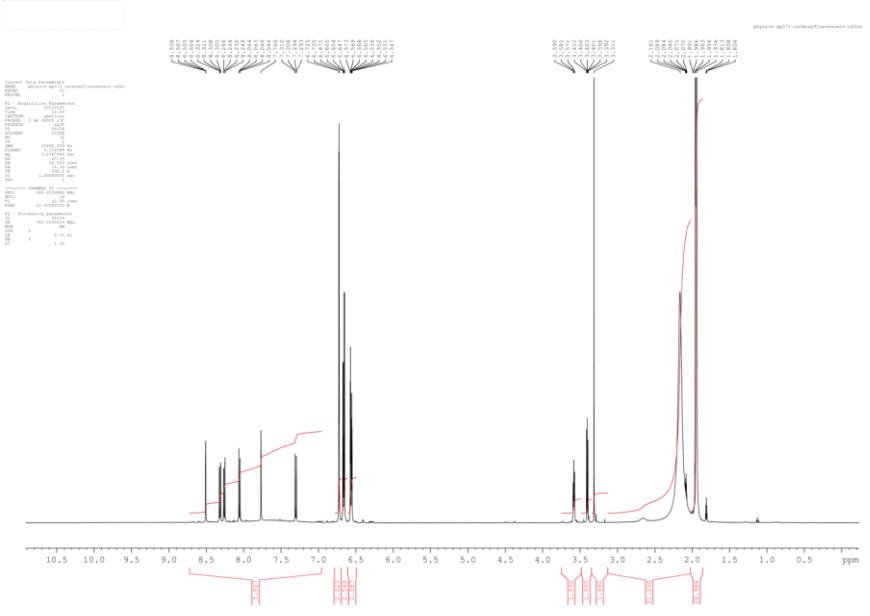

Figure S.3: ^{1}H NMR spectrum of **2** in deuterated acetonitrile.

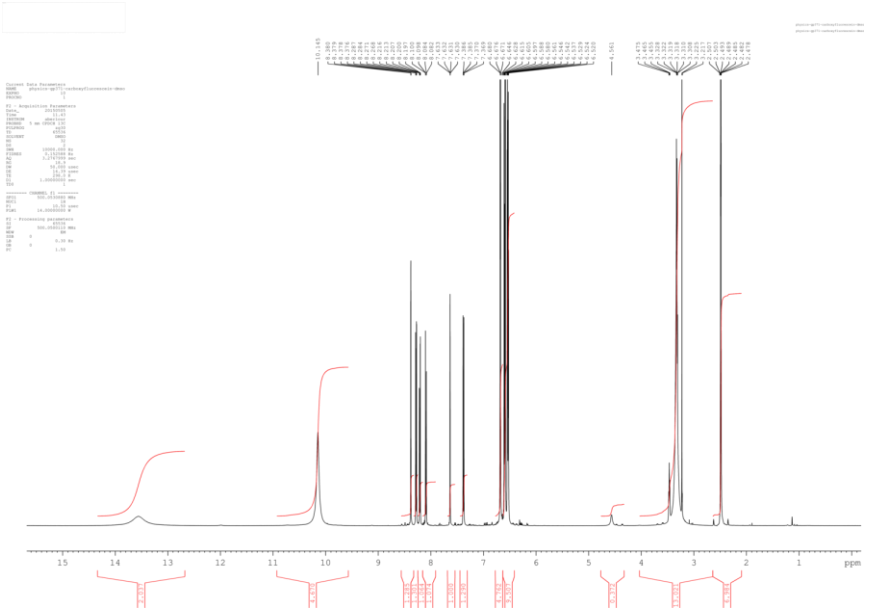

Figure S.4: ^{1}H NMR spectrum of **2** in deuterated dimethyl-sulfoxide.

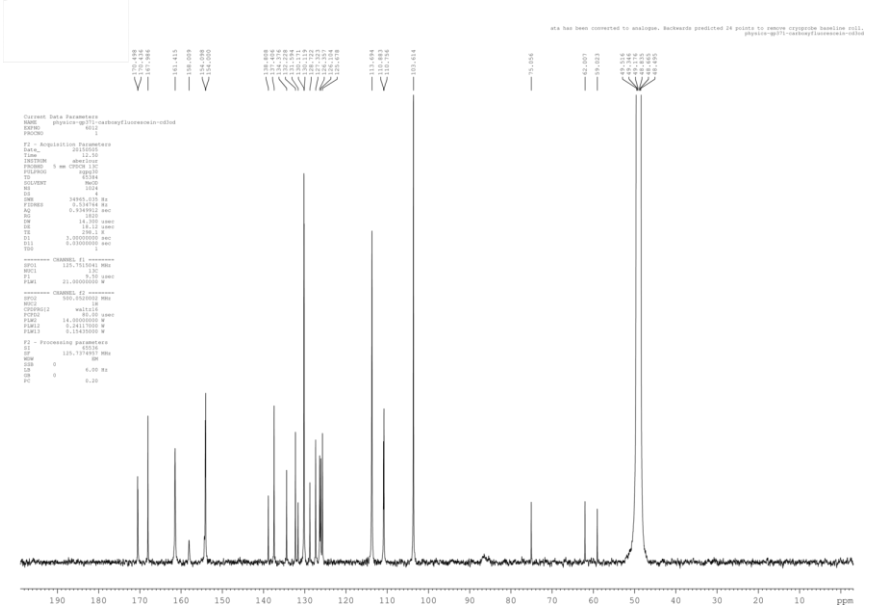

Figure S.5: ^{13}C{^{1}H} NMR spectrum of **2** in deuterated methanol.

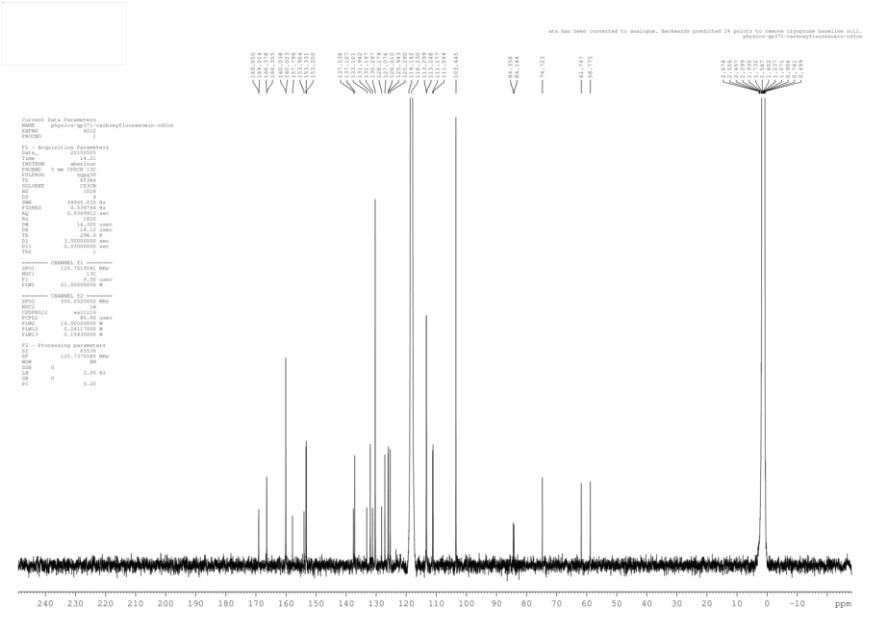

Figure S.6: $^{13}C\{^{1}H\}$ NMR spectrum of **2** in deuterated acetonitrile.

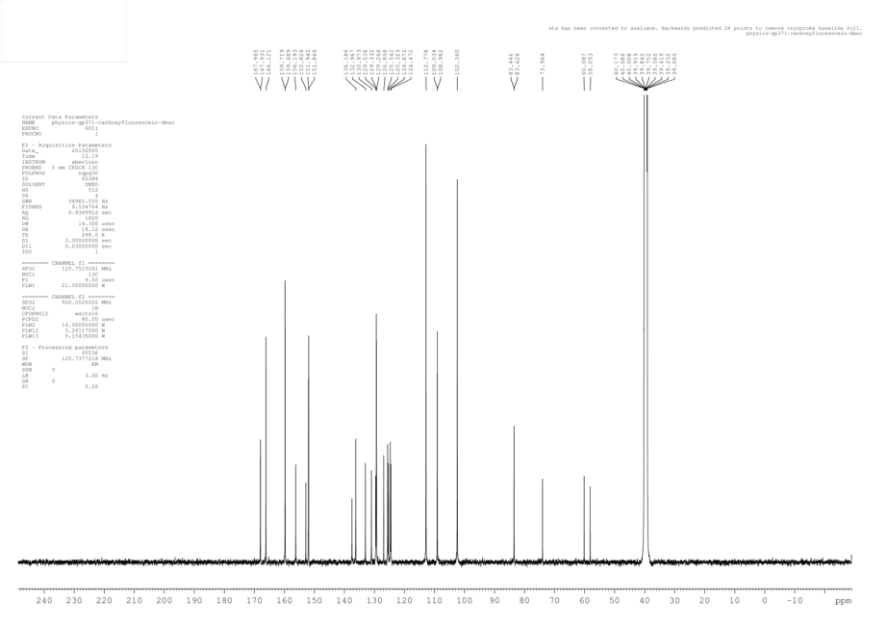

Figure S.7: $^{13}C\{^{1}H\}$ NMR spectrum of **2** in deuterated dimethyl-sulfoxide.

2 was examined by ^{1}H and $^{13}C\{^{1}H\}$ NMR spectroscopy in several solvents. The equilibrium in solution was influenced by the hydrogen-bond-donating (HBD) properties of the solvent. While protic solvents such as methanol are HBD solvents, aprotic solvents such as acetonitrile and DMSO are non-HBD solvents. The NMR analysis of **2** in methanol-d_4 (HBD), acetonitrile-d_3 (non-HBD), and DMSO-d_6 (non-HBD) showed that the HBD solvent methanol-d_4 interacted with the molecule creating an unaccounted chemical shift (δ = ~ 49 ppm), which is consistent with a tertiary carbocation. In contrast, for the very same atom a substantially different resonance (δ = ~ 84 ppm) is observed in non-HBD solvents acetonitrile-d3 and DMSO-d6.

S.3 UV/vis absorption spectroscopy

Spectral analysis of the optical absorption of this dye in a series of HBD and non-HBD solvents shows that solvent-interactions cause an additional component of the absorption spectrum in the visible region (~400-500 nm)(Figure S.7). This is caused by an interaction between solvent and molecules, in accordance with previous NMR results, but the present data is not sufficient to establish the exact cause of the additional absorption bands. The UV/vis spectrum of **2** in non-HBD solvents (acetonitrile, DMSO) did not exhibit any optical absorption in the visible region of the spectrum (Figure S.7). For the absorption band at 240 nm in **1**, **2**, and **5**, molar extinction coefficients of 2.50×10^{-4}, 2.92×10^{-4}, 3.20×10^{-4} L mol^{-1} cm^{-1} were measured, respectively.

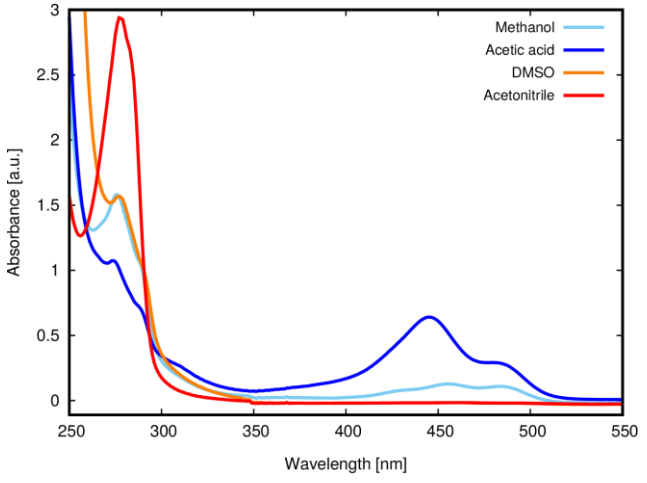

Figure S.8: UV/vis absorption spectra of the isomer mixture of **2** (0.04 mM) in methanol (HBD), acetic acid (HBD), DMSO (non-HBD), acetonitrile (non-HBD). In HBD solvents, isomer mixtures of **2** exhibit absorption in the visible region, while **2** in non-HBD solvents exhibits pre-dominant UV optical absorption.

S.4 Computational Studies

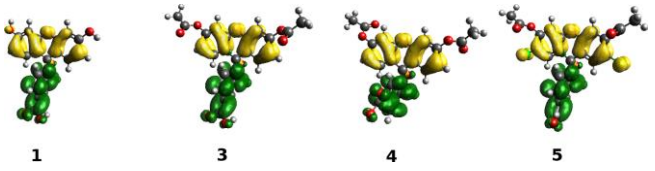

Figure S.9: Difference orbitals ($LUMO^2$-$HOMO^2$) of the parent dyes **1-5**, generated from DFT calculations at the PBE0 level of theory with 6-311+G(2d,p) basis set and PCM. Corresponding difference density orbitals are also generated by subtracting the square of the LUMO orbitals from the square of the HOMO orbitals. Increasing electron density is represented in green, while decreasing electron density is represented in yellow. Orbitals have been drawn at an isovalue of 0.0014.

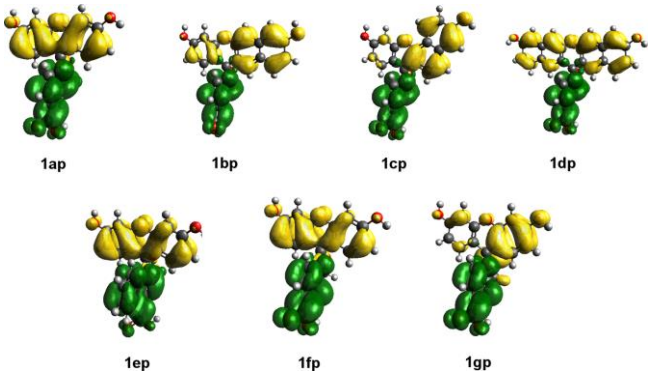

Figure S.10: Difference orbitals ($LUMO^2$-$HOMO^2$) of the parent dyes **1-5**, generated from DFT calculations at the PBE0 level of theory with 6-311+G(2d,p) basis set and PCM. Corresponding difference density orbitals are also generated by subtracting the square of the LUMO orbitals from the square of the HOMO orbitals. Increasing electron density is represented in green, while decreasing electron density is represented in yellow. Orbitals have been drawn at an isovalue of 0.0014.

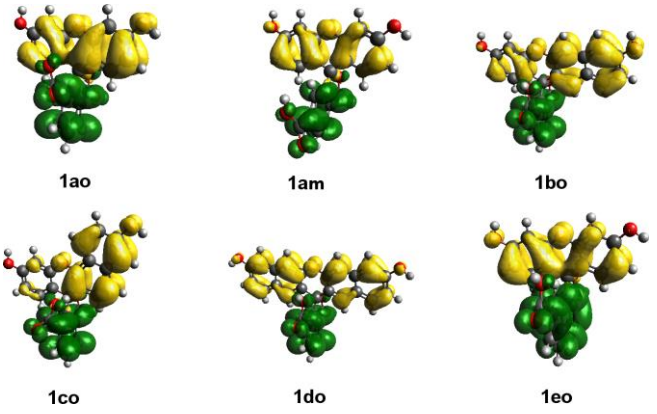

Figure S.11: Difference orbitals ($LUMO^2$-$HOMO^2$) of molecular engineered dyes with carboxylic acid at the ortho- and meta-position, generated from DFT calculations at the PBE0 level of theory with 6-311+G(2d,p) basis set and PCM. Corresponding difference density orbitals are also generated by subtracting the square of the LUMO orbitals from the square of the HOMO orbitals. Increasing electron density is represented in green, while decreasing electron density is represented in yellow. Orbitals have been drawn at an isovalue of 0.0007.

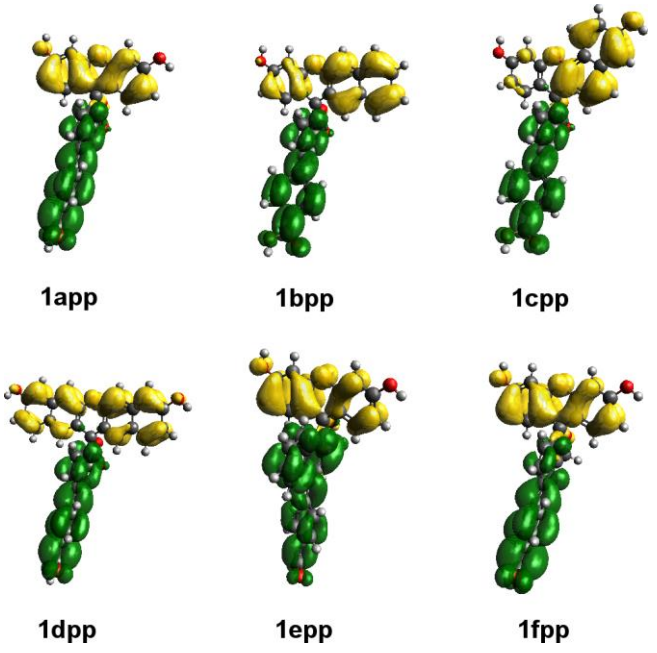

Figure S.12: Difference orbitals ($LUMO^2$-$HOMO^2$) of molecular engineered dyes with benzoic acid at the para-position, generated from DFT calculations at the PBE0 level of theory with 6-311+G(2d,p) basis set and PCM. Corresponding difference density orbitals are also generated by subtracting the square of the LUMO orbitals from the square of the HOMO orbitals. Increasing electron density is represented in green, while decreasing electron density is represented in yellow. Orbitals have been drawn at an isovalue of 0.0007.

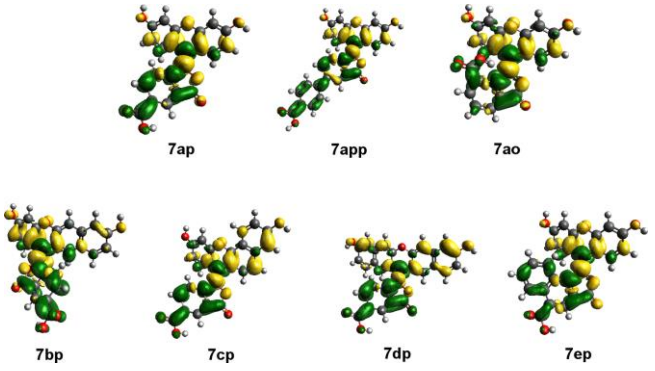

Figure S.13: Difference orbitals ($LUMO^2$-$HOMO^2$) of molecular engineered dyes of **7**, generated from DFT calculations at the PBE0 level of theory with 6-311+G(2d,p) basis set and PCM. Corresponding difference density orbitals are also generated by subtracting the square of the LUMO orbitals from the square of the HOMO orbitals. Increasing electron density is represented in green, while decreasing electron density is represented in yellow. Orbitals have been drawn at an isovalue of 0.0007.

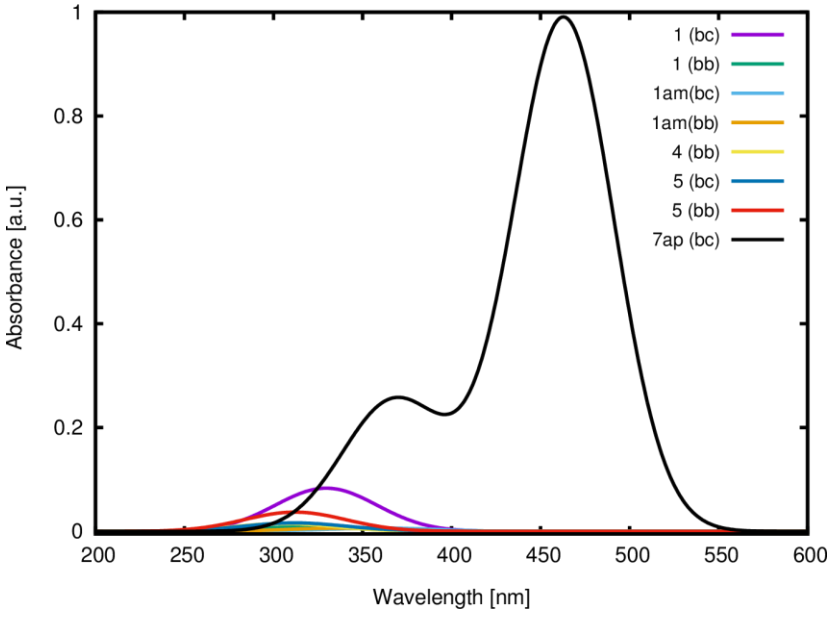

Figure S.14: Simulated optical absorption spectra of the dye···TiO_2 for the dyes studied at the TiO_2 interface. Excitation energies were calculated at the CAM-B3LYP level of theory and convoluted with a Gaussian window function to create the simulated spectra.

Table S.1: Initial atomic positions for DFT geometry optimization of the $(TiO_2)_9$ slab

Atom	x-position	y-position	z-position
Ti	15.6181	4.915257	15.538679
Ti	14.656039	6.531828	13.34211
Ti	17.613459	6.270851	13.08594
Ti	14.907321	7.679475	15.89544
Ti	20.75371	6.862666	12.242809
Ti	18.144937	4.270597	15.519405
Ti	20.762607	5.138394	14.77007
Ti	17.901846	7.483138	15.838273
Ti	21.136004	8.061333	15.539596
O	14.320878	4.940144	14.100751
O	16.506931	3.427434	16.089748
O	15.998929	6.52309	12.119939
O	16.415538	8.474763	16.506535
O	13.865553	7.895651	14.349067
O	14.579851	6.088665	16.664016
O	21.360157	5.298375	13.036662
O	17.128385	4.584195	13.950862
O	19.874559	3.641029	15.478823
O	19.05209	5.949794	14.72939
O	21.668387	6.23336	15.834641
O	18.97042	6.233881	11.96149
O	17.978321	8.085584	13.904925
O	20.702593	8.038422	13.60583
O	17.393451	5.716852	16.531218
O	22.237354	9.17945	15.984697
O	19.397398	8.19721	16.403101
O	16.051565	6.719305	14.671194